# Proximity of Bound Hoechst 33342 to the ATPase Catalytic Sites Places the Drug Binding Site of P-glycoprotein within the Cytoplasmic Membrane Leaflet†

Qin Qu and Frances J. Sharom*

*Guelph-Waterloo Centre for Graduate Work in Chemistry and Biochemistry, Department of Chemistry and Biochemistry, University of Guelph, Guelph, Ontario, Canada N1G 2W1*

*Received November 26, 2001*

ABSTRACT: The P-glycoprotein multidrug transporter carries out ATP-driven cellular efflux of a wide variety of hydrophobic drugs, natural products, and peptides. Multiple binding sites for substrates appear to exist, most likely within the hydrophobic membrane spanning regions of the protein. Since ATP hydrolysis is coupled to drug transport, the spatial relationship of the drug binding sites relative to the ATPase catalytic sites is of considerable interest. We have used a fluorescence resonance energy transfer (FRET) approach to estimate the distance between a bound substrate and the catalytic sites in purified P-glycoprotein. The fluorescent dye Hoechst 33342 (H33342), a high-affinity P-glycoprotein substrate, bound to the transporter and acted as a FRET donor. H33342 showed greatly enhanced fluorescence emission when bound to P-glycoprotein, together with a substantial blue shift, indicating that the drug binding site is located in a nonpolar environment. Cys428 and Cys1071 within the catalytic sites of P-glycoprotein were covalently labeled with the acceptor fluorophore NBD-Cl (7-chloro-4-nitrobenz-2-oxa-1,3-diazole). H33342 fluorescence was highly quenched when bound to NBD-labeled P-glycoprotein relative to unlabeled protein, indicating that FRET takes place from the bound dye to NBD. The distance separating the bound dye from the NBD acceptor was estimated to be ~38 Å. Transition-state P-glycoprotein with the complex ADP·orthovanadate·$Co^{2+}$ stably trapped at one catalytic site bound H33342 with similar affinity, and FRET measurements led to a similar separation distance estimate of 34 Å. Since previous FRET studies indicated that a fluorophore bound within the catalytic site was positioned 31−35 Å from the interfacial region of the bilayer, the H33342 binding site is likely located 10−14 Å below the membrane surface, within the cytoplasmic leaflet of the membrane, in both resting-state and transition-state P-glycoprotein.

Members of the ATP-binding cassette (ABC)[1] superfamily of membrane proteins are responsible for the ATP-dependent export or import of a wide range of solutes, from chloride ions to protein toxins, in organisms ranging from bacteria to human (*1*−*4*). Expression of one ABC protein, the P-glycoprotein multidrug transporter (Pgp), causes the phenomenon of multidrug resistance (MDR) in cultured cells and human tumors. Pgp is known to be responsible for the efflux of hundreds of structurally diverse hydrophobic compounds, including chemotherapeutic drugs, natural products, and peptides. The biochemistry and molecular pharmacology of Pgp have been discussed in several recent reviews (*5*−*7*).

The number, nature, and location of the drug binding sites of Pgp have been the subject of much speculation over the years. It is widely believed that substrates interact with the protein within the membrane itself, so that partitioning of the drug into the lipid bilayer becomes an important part of the overall transport process. Experimental evidence supporting this view includes the observation that esters of calcium indicator dyes never appear to reach the cytosol in MDR cells (*8*), and the finding that the binding affinity of several drugs to Pgp is highly correlated with their lipid/water partition coefficient (*9*). Cross-linking and other studies with engineered Cys residues have strongly suggested that the transmembrane (TM) regions of the protein, especially TM5, -6, -11 and -12, are directly involved in forming the drug binding site(s) (*10*, *11*).

Multiple drug binding sites appear to exist within the Pgp molecule. Dey et al. presented evidence for the existence of two nonidentical drug binding sites in the protein (*12*). This was supported by the observation of two-component quenching curves for binding of many drugs to purified Pgp reconstituted into lipid bilayers (*9*, *13*). Several research groups have also reported that transport of one substrate can be stimulated by binding of another substrate, suggesting that the two (or more) binding sites concerned are linked in a positive allosteric fashion (*14*−*16*), and photoaffinity labeling of Pgp by certain drug derivatives can be enhanced by the presence of another substrate (see, for example, ref *17*).

† This work was supported by a grant to F.J.S. from the National Cancer Institute of Canada, with funds provided by the Canadian Cancer Society.

* Correspondence should be addressed to this author at the Department of Chemistry and Biochemistry, University of Guelph, Guelph, Ontario, Canada N1G 2W1. Phone: 519-824-4120, ext 2247; FAX: 519-766-1499; E-mail: sharom@chembio.uoguelph.ca.

[1] Abbreviations: ABC, ATP-binding cassette; CHAPS, 3-[(3-cholamidopropyl)dimethylammonio]-1-propanesulfonate; FRET, fluorescence resonance energy transfer; H33342, Hoechst 33342; MDR, multidrug resistance/resistant; Pgp, P-glycoprotein; NBD-Cl, 7-chloro-4-nitrobenz-2-oxa-1,3-diazole; TM, transmembrane.

10.1021/bi0120897 CCC: $22.00 
Published on Web 03/13/2002

Recent drug binding experiments with purified Pgp confirmed that these multiple drug binding sites can communicate with each other allosterically (*18*). Neyfakh and co-workers recently proposed that multidrug binding proteins and multidrug transporters make use of van der Waals forces and surface complementarity to bind their substrates within a flexible binding region (*19*, *20*). Such a region of the protein may allow many different drugs to interact with it in somewhat different ways, providing the observation of multiple sites. More definitive localization of one or more drug binding sites of Pgp would assist greatly in formulating detailed models of its mechanism of action.

Drug transport is powered by ATP hydrolysis at the two nucleotide binding domains of Pgp, which are located at the cytosolic face of the membrane. The two ATPase catalytic sites within the nucleotide binding domains show complete cooperativity, in that only one is active at any instant in time, and they are proposed to operate in an alternating fashion (*21*, *22*). Since ATP hydrolysis is coupled to drug transport, the spatial relationship of the drug binding sites relative to the ATPase catalytic sites is of considerable interest. Our laboratory has shown that the intrinsic Trp fluorescence of Pgp, which likely arises from residues within the TM regions of the protein, is highly quenched by drug substrates, and also by both fluorescent ATP derivatives and unmodified nucleotides (*13*). The characteristics of this quenching suggest that it arises from fluorescence resonance energy transfer (FRET) from Trp to the bound drug or nucleotide, which implies that the emitting Trp residues are located within transfer distance of both the drug binding sites and the ATP catalytic sites. Such a compact structure would be predicted for coupling of ATP hydrolysis to drug transport.

In the present work, we have used a FRET approach to estimate the distance between a bound substrate and the ATPase catalytic sites of purified Pgp. The fluorescent dye Hoechst 33342 (H33342), a high-affinity Pgp substrate, was used as the energy donor. The acceptor fluorophore, 7-chloro-4-nitrobenz-2-oxa-1,3-diazole (NBD-Cl), was covalently linked to a cysteine residue within the Walker A motif of the nucleotide binding domains of Pgp. The efficiency of energy transfer was used to estimate the distance separating H33342 within its drug binding site from NBD at the ATPase catalytic sites. This was carried out for both resting-state Pgp and transition-state Pgp with a vanadate nucleotide complex stably trapped at one active site. Interpreting the present results in the context of a previous FRET study leads to the conclusion that the H33342 binding site is located within the cytoplasmic leaflet of the membrane bilayer.

## MATERIALS AND METHODS

*Materials*. 3-[(3-Cholamidopropyl)dimethylammonio]-1-propanesulfonate (CHAPS), disodium ATP, NBD-Cl, and sodium orthovanadate were purchased from Sigma Chemical Co. (St. Louis, MO). H33342 was obtained from Molecular Probes (Eugene, OR).

*Plasma Membrane Preparation and Pgp Purification*. Plasma membrane vesicles were isolated from MDR $CH^R$-B30 Chinese hamster ovary cells as described previously (*23*). Membrane vesicles were stored at −70 °C for no more than 3 months before use. Pgp was purified from $CH^RB30$ plasma membrane by the initial extraction of plasma membrane with 25 mM CHAPS buffer, followed by solubilization of the $S_1$ pellet in 15 mM CHAPS buffer, as described previously (*24*). Pgp was further purified by affinity chromatography on a Concanavalin A−Sepharose column. The final product consisted of 90−95% pure Pgp in 2 mM CHAPS/50 mM Tris-HCl/0.15 M NaCl/5 mM $MgCl_2$ (pH 7.5). The purified Pgp preparation was kept on ice and used within 24 h. Protein was quantitated by the method of Bradford (*25*) for plasma membrane, and by the method of Peterson (*26*) for purified Pgp, using bovine serum albumin (crystallized and lyophilized, Sigma) as a standard.

*Measurement of Pgp ATPase Activity*. $Mg^{2+}$-ATPase activity of Pgp was determined by measuring the release of inorganic phosphate from ATP. Purified Pgp was incubated with assay buffer (50 mM Tris-HCl/0.15 M NaCl/5 mM $MgCl_2$, pH 7.5), in the presence of 1 mM ATP at 37 °C for 5 min, as described earlier (*27*, *28*).

*Vanadate Trapping of Purified Pgp and Reactivation of Pgp ATPase Activity*. A stock solution of 100 mM sodium orthovanadate was prepared at pH 10, and aliquots were boiled for 4 min before each use to degrade polymeric species. A ∼100 μg aliquot of Pgp was incubated at 37 °C in a total volume of 1 mL of CHAPS buffer (2 mM CHAPS/50 mM Tris-HCl/0.15 M NaCl, pH 7.5) in the presence of 5 mM $CoCl_2$, 1 mM ATP, and 0.2 mM vanadate. After 20 min, the mixture was eluted through a Bio-Gel-P6 gel filtration column (Bio-Rad Laboratories, Mississauga, ON) preequilibrated with 2 mM CHAPS buffer. To measure reactivation of the ATPase activity of purified Pgp following vanadate trapping, the eluate containing Pgp was incubated at 22 °C, and at various times, aliquots were removed, and the ATPase activity was determined as described above.

*Double and Single Labeling of Purified Pgp with NBD-Cl*. Purified Pgp (∼800 μg) was incubated with 1 mM NBD-Cl at 22 °C for 1 h in the dark. Protein labeled with NBD-Cl at both NB domains (Pgp-2NBD) was obtained by removal of unreacted NBD-Cl using a Bio-Gel P-6 gel filtration column equilibrated with 2 mM CHAPS buffer. To prepare vanadate-trapped protein labeled with NBD-Cl at only one NB domain (Pgp-$V_i$-1NBD), ∼1000 μg of purified Pgp was incubated in a total volume of 2 mL of 2 mM CHAPS buffer containing 5 mM $CoCl_2$ at 37 °C for 20 min, in the presence of 1 mM ATP and 0.2 mM sodium orthovanadate. After incubation, the sample was eluted through a gel filtration column of Bio-Gel-P6 to remove excess ATP, vanadate, $CoCl_2$, and inorganic phosphate. The eluate was incubated with 1 mM NBD-Cl at 22 °C for 1 h in the dark. To remove unreacted NBD-Cl, the sample was passed through a Bio-Gel-P6 gel filtration column preequilibrated with 2 mM CHAPS buffer. Unlabeled Pgp was used as control for comparison to Pgp-$V_i$-1NBD and Pgp-2NBD. Sample protein concentrations were adjusted to 100 or 300 μg/mL, depending on the experiment.

*Fluorescence Measurements*. Fluorescence spectra were recorded on a PTI Alphascan-2 spectrofluorometer (Photon Technology International, London, ON, Canada) with the cell holder thermostated at 22 °C. All spectra were measured with a 2 nm excitation and emission band-pass. Emission spectra of labeled Pgps were corrected using a built-in automatic correction system. The measured fluorescence intensity was corrected for light scattering using controls containing unlabeled Pgp. In the case of fluorescence

quenching titrations, the inner filter effect was corrected at both the excitation and emission wavelengths as described previously (*24*, *29*, *30*), using the equation:

$$F_{i\mathrm{cor}} = (F_i - B)(V_i/V_0)10^{0.5b(A_{\lambda\mathrm{ex}}+A\lambda_{\mathrm{em}})} \quad (1)$$

where $F_{i\mathrm{cor}}$ is the corrected value of the fluorescence intensity, $F_i$ is the experimentally measured fluorescence intensity, $B$ is the background fluorescence intensity caused by scattering, $V_0$ is the initial volume of the sample, $V_i$ is the volume of the sample at a given point in the titration, $b$ is the path length of the optical cell in centimeters, and $A_{\lambda\mathrm{ex}}$ and $A_{\lambda\mathrm{em}}$ are the absorbance of the sample at the excitation and emission wavelengths, respectively.

In the case of titration of H33342 fluorescence enhancement, the following equation was used:

$$F_{i\mathrm{cor}} = (F_i - B_i)(V_i/V_0)10^{0.5b(A_{\lambda\mathrm{ex}}+A\lambda_{\mathrm{em}})} \quad (2)$$

where $B_i$ is the fluorescence intensity of free H33342 in 2 mM CHAPS buffer.

*Determination of Affinity of H33342 Binding to Pgp.* The affinity of H33342 binding to native Pgp, Pgp-$V_i$-1NBD, and Pgp-2NBD was estimated using two different approaches. The first method used quenching of the intrinsic Trp fluorescence of the protein, as described previously for other Pgp substrates (*13*). Briefly, a fixed concentration of purified Pgp was titrated at 22 °C with increasing concentrations of H33342. Trp residues were excited at 280 nm, and after each addition of H33342, the fluorescence was monitored at 325 nm. A control titration was carried out with 2 mM CHAPS buffer, and the data were corrected accordingly. Quenching of Trp fluorescence at various H33342 concentrations was fitted to the following equation, using SigmaPlot (SPSS Inc., Chicago IL):

$$\Delta F/F_0 \times 100 = \frac{(\Delta F_{\mathrm{max}}/F_0 \times 100) \times [\mathrm{S}]}{K_\mathrm{d} + [\mathrm{S}]} \quad (3)$$

where $(\Delta F/F_0 \times 100)$ represents the percent change in fluorescence intensity relative to the initial value after addition of H33342 at a concentration [S], $(\Delta F_{\mathrm{max}}/F_0 \times 100)$ is the maximum percent quenching of the fluorescence intensity that occurs upon saturation of the drug binding site, and $K_\mathrm{d}$ is the dissociation constant for binding of H33342 to Pgp. Fitting was performed by regression analysis using SigmaPlot, and values of $K_\mathrm{d}$ and $\Delta F_{\mathrm{max}}$ were extracted.

In the second approach, the affinity of H33342 binding to native Pgp, Pgp-$V_i$-1NBD, and Pgp-2NBD was estimated by FRET from Trp residues to the bound dye. A fixed concentration of purified Pgp was titrated with increasing concentrations of H33342. Excitation of Trp residues was carried out at 280 nm, whereas emission was monitored at the emission maximum for H33342. A control titration was carried out with 2 mM CHAPS buffer, and the data were corrected accordingly. The enhancement of H33342 fluorescence was computer-fitted to the following equation:

$$\Delta F = \frac{\Delta F_{\mathrm{max}} \times [\mathrm{S}]}{K_\mathrm{d} + [\mathrm{S}]} \quad (4)$$

where $\Delta F$ represents the increase in fluorescence intensity relative to the initial value after addition of H33342 at a concentration [S] and $\Delta F_{\mathrm{max}}$ is the maximum enhancement in fluorescence intensity that occurs upon saturation of the drug binding site, and a value for $K_\mathrm{d}$ was estimated.

*Energy Transfer from Bound H33342 to NBD at the Catalytic Sites*. To demonstrate FRET from bound H33342 to the NBD probe covalently linked to Cys residues at the catalytic sites, a fixed concentration of Pgp labeled with NBD-Cl (Pgp-2NBD) was titrated at 22 °C with increasing concentrations of H33342. The enhancement of H33342 fluorescence at 460 nm was measured, with excitation at 350 nm. Titration of purified unlabeled Pgp with H33342 was also carried out. Control titrations with H33342 were performed in buffer in the absence of Pgp, and the fluorescence intensities were subtracted from those recorded in the presence of Pgp and Pgp-2NBD. Enhancements of H33342 fluorescence at various concentrations were fitted to eq 4 above.

*Measurement of Quantum Yield.* The quantum yield, $Q_\mathrm{f}$, of H33342 free in 2 mM CHAPS buffer was determined relative to a standard, using a polarizer oriented at the magic angle (54.7°) in both the excitation and emission beams. The fluorescence emission spectra of H33342 and a solution of quinine sulfate in 0.1 N $H_2SO_4$ were measured using an excitation wavelength of 350 nm. Both the sample and standard had absorbance values less than 0.095 at 350 nm. The quantum yield of H33342 free in buffer, $Q_\mathrm{f}$, was calculated using the equation:

$$Q_\mathrm{f} = \frac{F_{\mathrm{H33342}}}{F_{\mathrm{quinine}}} \times \frac{A_{\mathrm{quinine}}}{A_{\mathrm{H33342}}} \times Q_{\mathrm{quinine}} \quad (5)$$

where $Q_{\mathrm{quinine}}$, the quantum yield of quinine, is known to be 0.51 in 0.1 N $H_2SO_4$, $F_{\mathrm{H33342}}$ and $F_{\mathrm{quinine}}$ are the integrals of the fluorescence of H33342 and quinine sulfate in the wavelength range 360−650 nm, respectively, and $A_{\mathrm{H33342}}$ and $A_{\mathrm{quinine}}$ are the absorbances of H33342 and quinine sulfate at 350 nm, respectively. The quantum yield of H33442 free in buffer was estimated to be 0.0205.

The quantum yield for H33342 bound to Pgp, $Q_\mathrm{b}$, was calculated by using the equation (*31*):

$$Q_\mathrm{b} = \frac{Q_\mathrm{f}}{[\mathrm{S}]_\mathrm{b}} \times \left(\frac{[\mathrm{S}]_\mathrm{t} F_{\mathrm{Pgp}}}{F_0} - [\mathrm{S}]_\mathrm{f}\right) \quad (6)$$

where $Q_\mathrm{f}$ is the quantum yield of H33342 free in buffer, $[\mathrm{S}]_\mathrm{b}$, $[\mathrm{S}]_\mathrm{f}$, and $[\mathrm{S}]_\mathrm{t}$ are the concentrations of bound H33342, free H33342, and total H33342, respectively, and $F_{\mathrm{Pgp}}$ and $F_0$ are fluorescence emission intensities of H33342 in the presence and absence of Pgp, respectively.

$[\mathrm{S}]_\mathrm{b}$ and $[\mathrm{S}]_\mathrm{f}$ are calculated as follows:

$$2[S]_\mathrm{b} = ([\mathrm{Pgp}] + K_\mathrm{d} + [\mathrm{S}]_\mathrm{t}) - \{([\mathrm{Pgp}] + K_\mathrm{d} + [\mathrm{S}]_\mathrm{t})^2 - 4[\mathrm{Pgp}][\mathrm{S}]_\mathrm{t}\}^{1/2} \quad (7)$$

$$[S]_\mathrm{f} = [S]_\mathrm{t} - [S]_\mathrm{b} \quad (8)$$

where [Pgp] is the Pgp concentration in micromolar. This equation is derived from the equation for equilibrium binding of H33342 to Pgp; Pgp + H33342 $\rightleftarrows$ Pgp·H33342.

*Determination of Parameters for FRET Analysis.* The efficiency of resonance energy transfer, $E$, between the donor

(H33342) and acceptor (NBD) can be written in terms of the quantum yield as

$$E = 1 - \frac{Q_{DA}}{Q_D} \tag{9}$$

where $Q_{DA}$ and $Q_D$ are the quantum yields of Pgp-bound H33342 ($Q_b$) in the presence and absence of the NBD acceptor.

The efficiency of FRET is related to the inverse sixth power of the distance, $R$, between the donor and acceptor in an isolated donor−acceptor system:

$$R = R_0(E^{-1} - 1)^{1/6} \tag{10}$$

where $R_0$ is the distance in angstroms at which the efficiency of energy transfer is 50%. $R_0$ can be calculated from

$$R_0 = (9.8 \times 10^3)(J\kappa^2 Q_D n^{-4})^{1/6} \tag{11}$$

where $J$ is the spectral overlap integral between donor and acceptor in units of $cm^3\ M^{-1}$, $Q_D$ is the fluorescence quantum yield of the donor, and $n$ is the refractive index of the medium between the chromophores, which was taken as 1.33, that of a dilute aqueous solution. The orientation factor, $\kappa^2$, was taken as 2/3.

The spectral overlap integral ($J$) was determined using the equation:

$$J = \frac{\int F_D(\lambda)\epsilon_A(\lambda)\lambda^4\,d\lambda}{\int F_D(\lambda)\,d\lambda} \tag{12}$$

where $F_D$ is the fluorescence intensity per unit wavelength interval in the presence of donor only, $\epsilon_A(\lambda)$ is the molar extinction coefficient of the acceptor, and $\lambda$ is the wavelength in centimeters. The fluorescence emission spectra of H33342 bound to Pgp were recorded using excitation at 350 nm, and the absorbance spectra of NBD-labeled Pgp were measured using a UV−visible spectrophotometer. $J$ was calculated from the spectral data using a computer program designed solely for that purpose by Dr. Uwe Oehler (Department of Chemistry and Biochemistry, University of Guelph).

*Measurement of Fluorescence Polarization*. The steady-state fluorescence anisotropy, $r$, and fluorescence polarization, $p$, are defined as follows (using T-format measurement on the spectrofluorometer):

$$r = \frac{I_{VV} - G \times I_{VH}}{I_{VV} + 2G \times I_{VH}} \tag{13}$$

$$p = 3r/(r + 2) \tag{14}$$

where $I_{VV}$ and $I_{VH}$ are the fluorescence intensities when the excitation polarizer is oriented in the vertical direction, and the emission polarizer is oriented in vertical and horizontal directions, respectively. The $G$-factor is the ratio of the sensitivities of the detection system for vertically and horizontally polarized light. $G$ was measured as

$$G = \frac{I_{HV}}{I_{HH}} \tag{15}$$

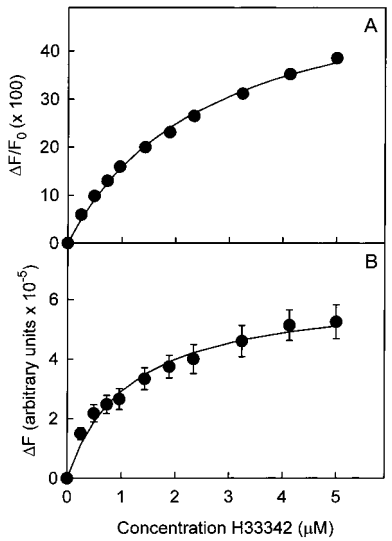


FIGURE 1: Determination of the affinity of binding of H33342 to Pgp using fluorescence techniques. (A) Quenching of the intrinsic Trp fluorescence of Pgp by binding of H33342. A solution of Pgp (120 $\mu$g/mL protein) in buffer consisting of 2 mM CHAPS/50 mM Tris-HCl/0.15 M NaCl, pH 7.5, was titrated with increasing concentrations of H33342 at 22 °C. Fluorescence emission was monitored at 325 nm (the emission maximum for Pgp Trp residues), following excitation at 280 nm. (B) Enhancement of H33342 emission resulting from energy transfer from Trp residues. A solution of Pgp in 2 mM CHAPS buffer (120 $\mu$g/mL protein) was titrated with increasing concentrations of H33342 at 22 °C. Trp residues were excited at 280 nm, and sensitized emission from H33342 was monitored at 480 nm. Where error bars are not visible, they are contained within the symbols.

where $I_{HV}$ and $I_{HH}$ are the fluorescence intensities when the excitation polarizer is oriented in the horizontal direction, and the emission polarizer is oriented in vertical and horizontal directions, respectively.

## RESULTS

*High-Affinity Interaction of H33342 with Pgp.* The lipophilic fluorescent dye H33342 was previously reported to be transported by Pgp in plasma membrane vesicles (*32*) and reconstituted lipid bilayers (*33*). To determine the affinity of binding of H33342 to native and NBD-labeled Pgp, two different approaches were used. The first method used quenching of the intrinsic Trp fluorescence of Pgp upon H33342 binding, as described previously for other substrates (*13*). Pgp was purified from the plasma membrane of the highly drug-resistant cell line $CH^RB30$ by a two-step solubilization procedure using the detergent CHAPS, followed by removal of contaminating glycoproteins by Concanavalin A−Sepharose chromatography (*24*). Titration of the purified protein with H33342 led to concentration-dependent, saturable quenching of the Trp fluorescence (Figure 1A). Fitting of the quenching data to an equation for a single binding site (eq 3; see Materials and Methods) led to an estimated dissociation constant, $K_d$, of 2.61 $\mu$M, indicating that the dye is a relatively high-affinity substrate for Pgp. The maximal fluorescence quenching at saturation with H33342 estimated from the computer fitting was 57.2 ± 2.0%. We previously proposed that the quenching of Pgp Trp residues upon binding of substrates arose from energy transfer from Trp to the bound drug (*13*). If this is indeed the case, then we would expect enhanced fluorescence

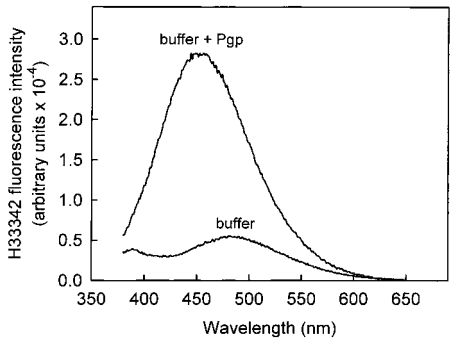


FIGURE 2: Fluorescence emission spectrum of H33342 ($\lambda_{ex}$ = 350 nm) at a concentration of 0.2475 $\mu$M, in 2 mM CHAPS buffer, and in the same buffer in the presence of 120 $\mu$g/mL Pgp. The wavelength of maximum emission is blue-shifted by ~22 nm in buffer with added Pgp, relative to buffer alone.

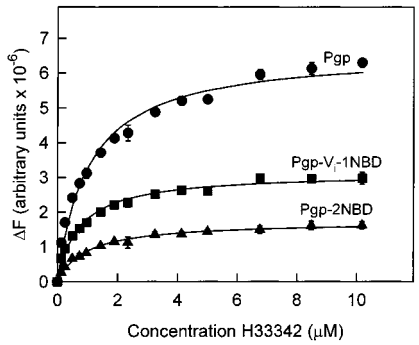


FIGURE 3: Enhancement of H33342 fluorescence following interaction with unlabeled Pgp (●), Pgp-$V_i$-1NBD (■), and Pgp-2NBD (▲). Pgp solutions (300 $\mu$g/mL protein) were titrated with increasing concentrations of H33342 at 22 °C, and enhancement of the fluorescence emission of the dye was measured at 460 nm following excitation at 350 nm. The same batch of Pgp was used for all three titration curves. Where error bars are not visible, they are contained within the symbols.

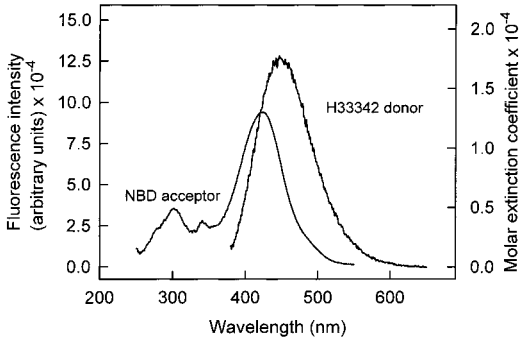


FIGURE 4: Spectral overlap between H33342 and Pgp-2NBD. Fluorescence emission spectrum of H33342 ($\lambda_{ex}$ = 350 nm), and the UV−visible absorption spectrum of Pgp labeled with NBD-Cl at both nucleotide binding domains (Pgp-2NBD).

emission of H33342 following excitation of Trp residues. Figure 1B shows that energy transfer takes place from Trp residues to bound H33342; excitation at 280 nm (the $\lambda_{max}$ for Trp excitation) resulted in enhanced fluorescence at the emission maximum for H33342. The enhancement was saturable and concentration-dependent, and could be fitted to a binding equation (eq 4) with a $K_d$ of 1.14 $\mu$M, very close to the dissociation constant measured above for Trp quenching. The fact that FRET takes place indicates that the binding site where H33342 interacts with Pgp is close to one or more of the emitting Trp residues within the TM regions of the transporter.

*H33342 Fluorescence Is Enhanced upon Interaction with Pgp at a Hydrophobic Binding Site*. In aqueous solution, H33342 has minimal fluorescence, which is enhanced when it is transferred to a nonpolar environment (*34*). The intensity of H33342 fluorescence emission was very low when measured in buffer containing 2 mM CHAPS. However, when H33342 was added to the same buffer containing purified Pgp, the fluorescence intensity increased dramatically, as shown in Figure 2. In addition, there was a large blue shift in the H33342 maximum emission wavelength, $\lambda_{em}$, from 480 nm in buffer alone to 458 nm in buffer containing purified Pgp, which indicates that the dye moved into a much more nonpolar environment in the presence of the transporter. This shift likely represents interaction of the dye with one of the drug binding sites of Pgp, which are located within the hydrophobic TM regions of the protein.

When unlabeled Pgp was titrated with H33342, it was evident that the fluorescence enhancement observed when the dye binds to the transporter was both concentration-dependent and saturable (Figure 3, upper curve). Fitting of the fluorescence enhancement data to a binding equation (eq 4) led to an estimate for $K_d$ of 1.05 $\mu$M. This value is very close to the $K_d$ values obtained by Trp quenching, and FRET from Trp residues to H33342 (see above), confirming that the fluorescence enhancement arises directly from interaction of the dye with the Pgp drug binding site.

*FRET between Bound H33342 and the NBD Probe at the Nucleotide Binding Domains of Pgp.* To establish the spatial relationship between the drug binding site for H33342 and the ATPase catalytic sites, we used a FRET approach to estimate the distance between bound H33342 (the donor) and an acceptor fluorophore, NBD-Cl, covalently bound within the ATPase catalytic sites of Pgp. We previously showed that labeling of Pgp with NBD-Cl takes place selectively at two Cys residues (Cys428 and Cys1071), one within each of the Walker A motifs of the nucleotide binding folds, to give a doubly labeled protein, Pgp-2NBD (*35*). Figure 4 shows that the overlap between the fluorescence emission spectrum of bound H33342 and the absorption spectrum of Pgp-2NBD is good (see Table 1 for the value of the spectral overlap integral, *J*), making this donor−acceptor pair an excellent choice for FRET experiments. When H33342 was added to a solution of Pgp labeled with the fluorescent acceptor (Pgp-2NBD), the fluorescence emission of the dye was greatly reduced compared to the situation where H33342 was added to a solution of unlabeled Pgp (Figure 5), indicating that energy was being transferred from the H33342 donor to the NBD acceptors. Titration of Pgp-2NBD with H33342 led to substantially lower maximal enhancement of the dye fluorescence (Figure 3, lower curve). The affinity of the interaction appeared largely unchanged, with a $K_d$ of 0.88 $\mu$M estimated from the titration curve by computer fitting. Thus, labeling of Pgp with NBD-Cl at the two ATPase active sites does not affect the reversible interaction of H33342 with the drug binding site.

*Proximity of Bound H33342 to the NBD Probe at the Catalytic Sites.* The efficiency of energy transfer was calculated from the quantum yield of the H33342 donor in the absence (unlabeled Pgp) and presence (Pgp-2NBD) of the NBD acceptor (see eq 9). H33342 interacts reversibly with the drug binding site of Pgp, so calculation of the

Table 1: Quantum Yields and Efficiencies of Energy Transfer between the H33342 Donor in the Drug Binding Site and the NBD Acceptor in the Catalytic Sites of Pgp[a]

| | | quantum yield of H33342, $Q_D$ | | | | efficiency of energy transfer, $E$ (%), per NBD acceptor | |
|---|---|---|---|---|---|---|---|
| $J$ ($cm^3 M^{-1}$) | $R_0$ (Å) | buffer | Pgp | Pgp-2NBD | Pgp-$V_i$-1NBD | Pgp-2NBD | Pgp-$V_i$-1NBD |
| $2.53 \times 10^{-14}$ value of $R$: | 33.2 | $(0.0205 \pm 1.9) \times 10^{-3}$ | $0.282 \pm 0.022$ | $0.112 \pm 0.014$ | $0.148 \pm 0.017$ | $0.301 \pm 0.016$ 38.2 Å | $0.475 \pm 0.016$ 33.8 Å |

[a] Five independent experiments were carried out for determination of each value of $Q_D$, with different preparations of Pgp, Pgp-$V_i$-1NBD, and Pgp-2NBD in each case. Means ± SEM are indicated.

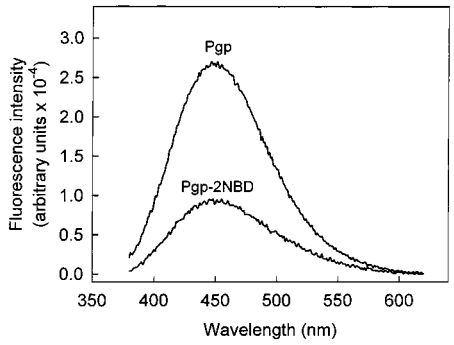


FIGURE 5: Quenching of H33342 fluorescence emission resulting from energy transfer to the NBD donor in resting-state Pgp. The fluorescence emission spectrum of H33342 at a concentration of 0.2475 $\mu$M was recorded following binding to unlabeled Pgp (100 $\mu$g/mL) or Pgp labeled at both nucleotide binding domains with NBD-Cl (Pgp-2NBD; 100 $\mu$g/mL). Excitation was carried out at 350 nm.

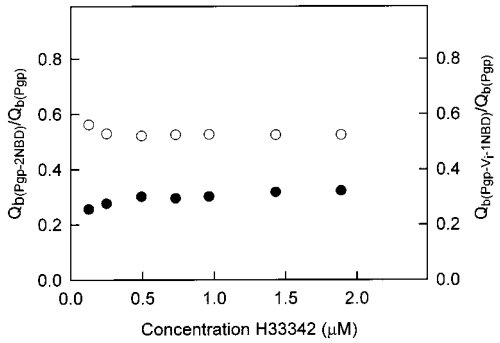


FIGURE 6: Ratio of the quantum yield of H33342 following binding to Pgp-2NBD (●) and Pgp-$V_i$-1NBD (○), relative to the quantum yield following binding to unlabeled Pgp, was measured at various H33342 concentrations. The ratio of $Q_b$ values remains approximately constant over a range of H33342 concentrations, reflecting various degrees of occupancy of the drug binding site.

quantum yield of H33342 bound to Pgp ($Q_b$), in the presence and absence of the acceptor, must take account of this equilibrium. $Q_b$ was calculated using eqs 6, 7, and 8 (see Materials and Methods), together with known concentrations of H33342 and Pgp, and the measured value of $K_d$ for H33342 binding to Pgp (see above). The ratio of the quantum yield of H33342 when bound to Pgp-2NBD relative to that when bound to native Pgp remained constant at ~0.30 over a range of drug concentrations (0−2 $\mu$M; Figure 6, lower curve). This indicates that the energy-transfer efficiency from H33342 to NBD was comparable no matter what the degree of occupancy of the drug binding site. The quantum yields of H33342 free in solution and bound to Pgp in the absence and presence of the NBD acceptor are shown in Table 1, together with the calculated efficiencies of energy transfer. The measured value of the efficiency of energy transfer from H33342 to Pgp-2NBD was halved, to give the energy-transfer efficiency per NBD acceptor (Table 1). To date, all the spectroscopic and kinetic evidence we have gathered indicates that the two nucleotide binding domains of Pgp behave identically, and a previous FRET study implied that they were also positioned symmetrically with respect to the bilayer surface (*35*).

Estimation of $R$, the distance between the donor and acceptor, requires calculation of the value of $R_0$, the distance in angstroms at which the efficiency of energy transfer is 50%, for that particular donor−acceptor pair. Using eq 11 (see Materials and Methods), $R_0$ for H33342 and NBD was calculated to be ~33 Å (see Table 1). We estimated the value of $R$ to be 38.2 Å for H33342 bound to Pgp-2NBD (Table 1). A previous FRET study using Pgp labeled with a different fluorophore at the same Cys residues indicated that the fluorescent groups at the active site were located symmetrically with respect to the membrane surface (*35*). Distance measurements placed them 31−35 Å from the interfacial region of the bilayer, or 23.5−27.5 Å above the membrane surface (*35*). Thus, a measured $R$ value of ~38 Å indicates that the binding site for H33342 is positioned approximately 10−14 Å below the bilayer surface. This places the interaction site for the dye within the cytoplasmic leaflet of the membrane.

The value of the orientation factor, $\kappa^2$, was taken as 2/3, which represents the case where the donor and the acceptor both rotate rapidly relative to the donor fluorescence lifetime. As discussed previously (*36*), small differences between the true and assumed value of $\kappa^2$ give only small errors in the calculated distances. It has also been argued that the value of $\kappa^2$ is not an important issue, since the distances estimated by FRET for several proteins agree well with distances determined crystallographically (*37*). In addition, we calculated the maximum upper and lower bounds of the error in $R$ from the measured fluorescence polarization of the donor and acceptor, using the estimates computed by Haas et al. (*38*). Polarization experiments indicated that the values of $p$ for H33342 and NBD bound to Pgp were 0.41 and 0.46, respectively, giving a maximum error range of ±17% in $R$ by assuming a $\kappa^2$ value of 2/3.

*FRET between Bound H33342 and the NBD Probe in Transition-State Pgp*. To ascertain whether the distance separating the H33342 binding site from the NBD probe differs when Pgp progresses through the catalytic cycle from the resting state to enter the transition state, FRET experiments were carried out on Pgp with vanadate stably trapped in one catalytic site. Urbatsch et al. previously reported that addition of vanadate to Pgp in the presence of ATP and $Co^{2+}$ led to a long-lived complex with ADP·$V_i$·$Co^{2+}$ trapped in the active site of one nucleotide binding domain (*39*). We

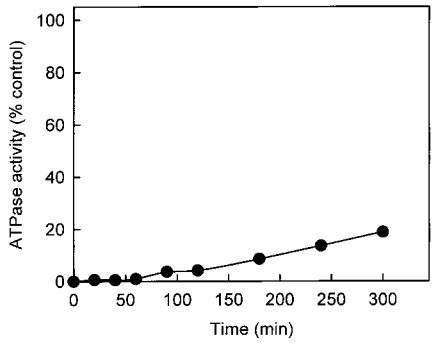


FIGURE 7: Reactivation of Pgp ATPase activity following trapping of ADP·$V_i$·$Co^{2+}$ in the catalytic site. Following removal of vanadate, the Pgp sample was incubated at 22 °C to allow release of trapped ADP·$V_i$·$Co^{2+}$ from the catalytic site. Pgp samples were removed at various times up to 5 h, and the ATPase activity was determined. Data are expressed as percent control relative to a sample of purified Pgp that was treated identically, but in the absence of vanadate.

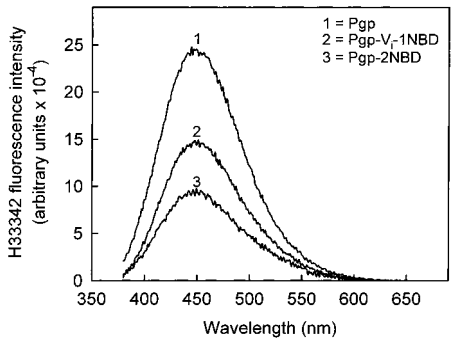


FIGURE 8: Quenching of H33342 fluorescence emission resulting from energy transfer to the NBD donor in Pgp-$V_i$-1NBD, compared to energy transfer to Pgp-2NBD. The fluorescence emission spectrum of H33342 at a concentration of 0.2475 $\mu$M was recorded following binding to unlabeled Pgp, Pgp-$V_i$-1NBD, or Pgp-2NBD, all at a protein concentration of 100 $\mu$g/mL. Excitation was carried out at 350 nm.

therefore used this approach to determine whether the site separation changed in the transition state. Addition of ATP to Pgp in the presence of $Co^{2+}$ led to rapid and complete inhibition of ATPase activity. The Pgp·ADP·$V_i$·$Co^{2+}$ complex was very stable, as indicated by the low rate of reactivation of the ATPase activity as ADP dissociates from the active site. As shown in Figure 7, when Pgp·ADP·$V_i$·$Co^{2+}$ was incubated at 22 °C, ATPase activity was barely detectable after 2 h, and only reached a level of 20% of control activity after a period of 5 h. Thus, there is sufficient time for several experimental manipulations while maintaining the trapped state. The stably trapped vanadate−$Co^{2+}$ complex of Pgp was labeled with NBD-Cl, to give Pgp-$V_i$-1NBD, followed by binding of H33342. The quantum yield of H33342 was higher when bound to Pgp-$V_i$-1NBD compared to Pgp-2NBD, thus resulting in higher overall fluorescence emission, because of the presence of only one acceptor fluorophore (Figure 6). $Q_b$ was relatively constant at ~0.52 over a range of drug concentrations (Figure 6, upper curve). As shown in Figure 3 (middle curve), the vanadate-trapped state of Pgp bound H33342 with similar affinity, 0.76 $\mu$M, compared to native Pgp and Pgp-2NBD. Energy transfer from the donor dye to the bound NBD acceptor was examined for the vanadate-trapped state. Figure 8 shows the H33342 fluorescence emission spectra for dye bound to unlabeled Pgp, Pgp-$V_i$-1NBD (transition-state Pgp), and Pgp-2NBD (resting-state Pgp). It is clear that the extent of quenching of the transition-state complex is lower than that of the resting-state protein, because of the presence of one NBD acceptor rather than two. However, the efficiency of energy transfer per NBD acceptor was higher than that measured for resting-state Pgp-2NBD (see Table 1). This led to a slightly lower estimate for $R$ of 33.8 Å (Table 1). Thus, the drug binding site also appears to be located within the cytoplasmic leaflet of the bilayer when Pgp is in the vanadate-trapped transition state.

## DISCUSSION

Fluorescence spectroscopic approaches have proved to be a very powerful tool in the study of Pgp (*40*−*42*), a transporter for which very little structural information is available from other sources. The affinity of drug and nucleotide binding has been quantitated by fluorescence quenching (*13*, *24*), and the proximity of the ATPase catalytic sites to the membrane surface (*35*) and their separation from each other (*43*) have been estimated using FRET approaches. In the present work, we have investigated the spatial relationship between the drug binding site where H33342 interacts, and the ATPase active sites within the nucleotide binding folds of Pgp.

The location of the drug binding site(s) of the Pgp multidrug transporter has been the object of much speculation. Recent work has provided indirect evidence that the drug binding region may be located within the cytoplasmic leaflet of the bilayer. Transport studies with the fluorescent dyes H33342 and LDS-751 suggested that they were likely extracted from the cytoplasmic leaflet of the membrane (*32*, *44*). Recent work by Ferry et al. (*45*) implied that the drug binding site for the permanently charged modulator derivative *N*-methyl-dexniguldipine was accessible only from the cytoplasmic face of the protein, and we have also reported that certain peptide modulators cannot interact with Pgp in intact cells if supplied on the extracellular side of the membrane, but can do so in membrane vesicle systems where the cytoplasmic face of the membrane is accessible (*46*). In the present study, direct FRET measurement of the distance separating bound H33342 from NBD probes in the catalytic sites clearly places the drug interaction site within the cytoplasmic membrane leaflet. The Pgp molecule appears to be structurally and functionally symmetrical with respect to the nucleotide binding domains. Vanadate is trapped equally in the N- and C-terminal halves of the protein (*47*), so that the species Pgp-$V_i$-1NBD will consist of a mixture of Pgp with the N-half trapped and Pgp with the C-half trapped. Thus, both Pgp-2NBD and Pgp-$V_i$-1NBD should behave symmetrically in FRET experiments; if any small differences do exist between the two halves, we will obtain an average of the FRET distance for each half.

The present work represents the first direct measurement of the location of the drug binding sites within Pgp relative to the other domains, and allows us to start building up a low-resolution FRET map of the protein. Figure 9 shows a simple model of the Pgp molecule, with distances that have been measured by FRET indicated. We recently showed that the two ATPase active sites were closely associated, with an estimated distance of 30 Å between the side chain S atoms

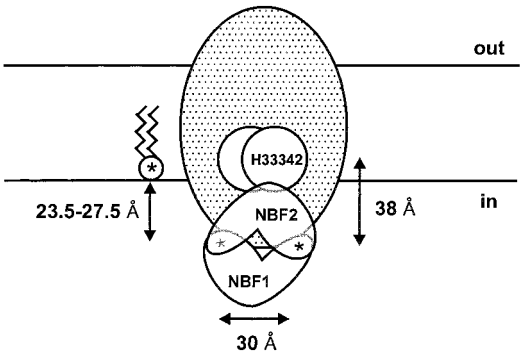


FIGURE 9: Low-resolution map of Pgp as determined by FRET. Experiments using a donor and acceptor covalently linked to the Walker A Cys residues within the two nucleotide binding folds NBF1 and NBF2 (*43*) place the S atoms ~30 Å apart, indicating that their separation is compatible with the X-ray crystal structure of Rad50cd (*48*). Each nucleotide binding domain is shown as contributing residues to the active site of the partner domain. A previous study in our laboratory localized the ATPase active sites of the nucleotide binding folds about 23.5−27.5 Å from the bilayer surface (*35*). The present study indicates that the binding site for H33342 is about 38 Å from the NBD fluorescent probe covalently bound to ATPase active site, placing it within the cytoplasmic leaflet of the membrane. The location of this site relative to the catalytic site is largely unchanged in the vanadate-trapped state. A second drug binding site is shown overlapping with the site for H33342; evidence for the existence of multiple drug binding sites is discussed in the text.

of the two Cys residues (*43*). This separation is compatible with the recently reported crystal structure of the Rad50cd dimer (*48*), but not with that of the HisP dimer (*49*). Accordingly, Figure 9 shows the two nucleotide binding domain aligned as in the Rad50cd dimer, with the C motif (ABC signature region) of each nucleotide binding domain contributing to the active site of the other domain in the dimer. Previous work indicated that the two active sites were symmetrically arranged relative to the membrane, about 23.5−27.5 Å away from the membrane surface (*35*), and thus the present work places the H33342 binding site 10−14 Å below the membrane surface. We currently do not know the orientation of the nucleotide binding domain dimer relative to the membrane.

The location of the drug binding site within the cytoplasmic leaflet of the membrane is also in accord with the original suggestion that Pgp may operate as a drug flippase (*50*). Evidence to support this view has grown in recent years. Pgp can act as a flippase for various fluorescent phospholipid derivatives in intact cells (*51*, *52*), and our laboratory recently demonstrated that Pgp reconstituted into proteoliposomes of defined phospholipids can translocate a number of phospholipid species and sphingomyelin from one lipid leaflet to the other (*53*). In contrast, Shapiro and co-workers have suggested that, while Pgp takes it substrates from the cytoplasmic leaflet, it delivers them to the external aqueous environment, rather than the other leaflet of the membrane (*32*). A more detailed examination of the process of drug transport using reconstituted systems will likely be necessary to resolve this issue.

Our results indicate that the site where H33342 interacts is also located within the cytoplasmic leaflet of the membrane when Pgp is trapped in a stable transition-state conformation using orthovanadate and $Co^{2+}$. The estimate of *R* is slightly smaller, placing the bound drug in the cytoplasmic leaflet, closer to the membrane surface by about 4 Å. Thus, our fluorescence data clearly indicate that H33342 is still bound within the cytoplasmic membrane leaflet at this stage of the catalytic cycle, and at approximately the same location within the cytoplasmic leaflet. Van Veen and co-workers have proposed that the bacterial multidrug transporter LmrA (which is closely related to Pgp) possesses two drug binding sites (*54*): a transport-competent site on the cytoplasmic membrane side of the membrane, and a drug-release site on the extracellular side of the membrane. The interconversion of these two sites is thought to occur via the catalytic transition-state intermediate, driven by ATP hydrolysis. The mechanism proposed for LmrA may also apply to Pgp and other ABC transporters (*55*). The results of the present study rule out mechanistic proposals for the transport process where the drug has already moved to the exofacial site in the transition state, or has been released from the binding site altogether. This suggests that prior dissociation of $P_i$ and/or ADP is necessary for drug relocation to take place. This conclusion is in agreement with the work of Senior et al., who have already suggested that the catalytic step most likely providing the energy to drive transport is dissociation of $P_i$ (*22*).

Based on photoaffinity labeling experiments using azido drug analogues, it has been proposed that Pgp has a very low affinity for drug substrates when in the vanadate-trapped transition state (*56*). This decrease in drug affinity was proposed to allow for release of the bound drug during the transport cycle. The results of the present study clearly show that H33342 is still bound to Pgp, with a similar high affinity, in the long-lived transition state formed by trapping with vanadate and $Co^{2+}$. We have also been able to demonstrate unchanged high-affinity binding of several other drugs to purified Pgp in the vanadate-trapped state (Q. Qu and F. J. Sharom, unpublished data). The efficiency of photoaffinity labeling (which is usually unknown) depends on protein conformation around the photoactive probe. Since the conformation of the vanadate-trapped state is known to be distinctly different from that of resting-state Pgp (*57*, *58*), it is likely that the observed lack of photolabeling in the trapped state reflects a change in protein conformation, rather than a real decrease in drug binding affinity. This type of effect has already been observed by Sankaran et al., who noted that, while 8-azido-ATP could be cross-linked to Pgp after transition-state trapping, in the case of 2-azido-ATP there was no covalent labeling in the trapped state (*59*). However, the 2-azido analogue bound to Pgp with the same affinity as assessed by inhibition experiments. They concluded that, in the trapped state, there are no suitable amino acid side chains adjacent to the photoactivated 2-position of bound 2-azido-ATP, whereas the reverse is true for the 8-azido analogue. Thus, caution should be used when interpreting photoaffinity experiments to assess binding affinities in the absence of additional independent information.

Using transport studies with H33342 and rhodamine123, Shapiro and Ling showed that certain classes of Pgp substrates displayed positive allosteric interactions, and they proposed the existence of two separate (possible overlapping) drug binding sites, which they designated the H site (for H33342) and the R site (for rhodamine123) (*15*). Rhodamine123 bound to the R site and stimulated H33342 transport via the H site, and H33342 bound to the H site

and stimulated rhodamine123 transport via the R site. These sites are clearly interconnected functionally, but the spatial relationship between them is unknown. Using transport measurements in reconstituted proteoliposomes containing Pgp, we have mapped the binding of many different drug substrates, a number of which are fluorescent, to the H or the R site (P. Lu and F. J. Sharom, unpublished data). Using the FRET approach described here, we have mapped the location of the H site; it should be possible to do the same for the R site, and to ascertain whether it is also located within the cytoplasmic leaflet of the membrane.

## REFERENCES


1. Doige, C. A., and Ames, G. F. (1993) *Annu. Rev. Microbiol. 47*, 291−319.
2. Van Veen, H. W., and Konings, W. N. (1998) *Biochim. Biophys. Acta 1365*, 31−36.
3. Holland, I. B., and Blight, M. A. (1999) *J. Mol. Biol. 293*, 381−399.
4. Jones, P. M., and George, A. M. (1999) *FEMS Microbiol. Lett. 179*, 187−202.
5. Sharom, F. J. (1997) *J. Membr. Biol. 160*, 161−175.
6. Ambudkar, S. V., Dey, S., Hrycyna, C. A., Ramachandra, M., Pastan, I., and Gottesman, M. M. (1999) *Annu. Rev. Pharmacol. Toxicol. 39*, 361−398.
7. Germann, U. A., and Chambers, T. C. (1998) *Cytotechnology 27*, 31−60.
8. Homolya, L., Hollo, Z., Germann, U. A., Pastan, I., Gottesman, M. M., and Sarkadi, B. (1993) *J. Biol. Chem. 268*, 21493−21496.
9. Romsicki, Y., and Sharom, F. J. (1999) *Biochemistry 38*, 6887−6896.
10. Loo, T. W., and Clarke, D. M. (1999) *Biochim. Biophys. Acta 1461*, 315−325.
11. Loo, T. W., and Clarke, D. M. (1999) *Biochem. Cell Biol. 77*, 11−23.
12. Dey, S., Ramachandra, M., Pastan, I., Gottesman, M. M., and Ambudkar, S. V. (1997) *Proc. Natl. Acad. Sci. U.S.A. 94*, 10594−10599.
13. Liu, R., Siemiarczuk, A., and Sharom, F. J. (2000) *Biochemistry 39*, 14927−14938.
14. Sharom, F. J., Yu, X., DiDiodato, G., and Chu, J. W. K. (1996) *Biochem. J. 320*, 421−428.
15. Shapiro, A. B., and Ling, V. (1997) *Eur. J. Biochem. 250*, 130−137.
16. Shapiro, A. B., Fox, K., Lam, P., and Ling, V. (1999) *Eur. J. Biochem. 259*, 841−850.
17. Safa, A. R., Roberts, S., Agresti, M., and Fine, R. L. (1994) *Biochem. Biophys. Res. Commun. 202*, 606−612.
18. Martin, C., Berridge, G., Higgins, C. F., Mistry, P., Charlton, P., and Callaghan, R. (2000) *Mol. Pharmacol. 58*, 624−632.
19. Zheleznova, E. E., Markham, P., Edgar, R., Bibi, E., Neyfakh, A. A., and Brennan, R. G. (2000) *Trends Biochem. Sci. 25*, 39−43.
20. Vazquez-Laslop, N., Zheleznova, E. E., Markham, P. N., Brennan, R. G., and Neyfakh, A. A. (2000) *Biochem. Soc. Trans. 28*, 517−520.
21. Senior, A. E., and Gadsby, D. C. (1997) *Semin. Cancer Biol. 8*, 143−150.
22. Senior, A. E., al-Shawi, M. K., and Urbatsch, I. L. (1995) *FEBS Lett. 377*, 285−289.
23. Doige, C. A., and Sharom, F. J. (1991) *Protein Expression Purif. 2*, 256−265.
24. Liu, R., and Sharom, F. J. (1996) *Biochemistry 35*, 11865−11873.
25. Bradford, M. M. (1976) *Anal. Biochem. 72*, 248−254.
26. Peterson, G. L. (1977) *Anal. Biochem. 83*, 346−356.
27. Doige, C. A., Yu, X., and Sharom, F. J. (1992) *Biochim. Biophys. Acta 1109*, 149−160.
28. Sharom, F. J., Yu, X., Chu, J. W. K., and Doige, C. A. (1995) *Biochem. J. 308*, 381−390.
29. Lakowicz, J. R. (1999) in *Principles of Fluorescence Spectroscopy*, Kluwer Academic Publishers, New York.
30. Parker, C. A. (1968) in *Photoluminescence of Solutions*, Elsevier Publishing Co., Amsterdam.
31. Cerione, R. A., and Hammes, G. G. (1982) *Biochemistry 21*, 745−752.
32. Shapiro, A. B., and Ling, V. (1997) *Eur. J. Biochem. 250*, 122−129.
33. Shapiro, A. B., Corder, A. B., and Ling, V. (1997) *Eur. J. Biochem. 250*, 115−121.
34. Shapiro, A. B., and Ling, V. (1995) *J. Biol. Chem. 270*, 16167−16175.
35. Liu, R., and Sharom, F. J. (1998) *Biochemistry 37*, 6503−6512.
36. Dale, R. E., Eisinger, J., and Blumberg, W. E. (1979) *Biophys. J. 26*, 161−193.
37. dos Remedios, C. G., and Moens, P. D. (1995) *J. Struct. Biol. 115*, 175−185.
38. Haas, E., Katchalski-Katzir, E., and Steinberg, I. Z. (1978) *Biochemistry 17*, 5064−5070.
39. Urbatsch, I. L., Sankaran, B., Weber, J., and Senior, A. E. (1995) *J. Biol. Chem. 270*, 19383−19390.
40. Sharom, F. J., Liu, R., and Romsicki, Y. (1998) *Biochem. Cell Biol. 76*, 695−708.
41. Sharom, F. J., Liu, R., Romsicki, Y., and Lu, P. (1999) *Biochim. Biophys. Acta 1461*, 327−345.
42. Sharom, F. J., Liu, R., Qu, Q., and Romsicki, Y. (2001) *Semin. Cell Dev. Biol. 12*, 257−266.
43. Qu, Q., and Sharom, F. J. (2001) *Biochemistry 40*, 1413−1422.
44. Shapiro, A. B., and Ling, V. (1998) *Eur. J. Biochem. 254*, 181−188.
45. Ferry, D., Boer, R., Callaghan, R., and Ulrich, W. R. (2000) *Int. J. Clin. Pharmacol. Ther. 38*, 130−140.
46. Sharom, F. J., Lu, P., Liu, R., and Yu, X. (1998) *Biochem. J. 333*, 621−630.
47. Urbatsch, I. L., Sankaran, B., Bhagat, S., and Senior, A. E. (1995) *J. Biol. Chem. 270*, 26956−26961.
48. Hopfner, K. P., Karcher, A., Shin, D. S., Craig, L., Arthur, L. M., Carney, J. P., and Tainer, J. A. (2000) *Cell 101*, 789−800.
49. Hung, L. W., Wang, I. X., Nikaido, K., Liu, P. Q., Ames, G. F., and Kim, S. H. (1998) *Nature 396*, 703−707.
50. Higgins, C. F., and Gottesman, M. M. (1992) *Trends Biochem. Sci. 17*, 18−21.
51. van Helvoort, A., Smith, A. J., Sprong, H., Fritzsche, I., Schinkel, A. H., Borst, P., and van Meer, G. (1996) *Cell 87*, 507−517.
52. van Helvoort, A., Giudici, M. L., Thielemans, M., and van Meer, G. (1997) *J. Cell Sci. 110*, 75−83.
53. Romsicki, Y., and Sharom, F. J. (2001) *Biochemistry 40*, 6937−6947.
54. Van Veen, H. W., Margolles, A., Müller, M., Higgins, C. F., and Konings, W. N. (2000) *EMBO J. 19*, 2503−2514.
55. Van Veen, H. W., Higgins, C. F., and Konings, W. N. (2001) *Res. Microbiol. 152*, 365−374.
56. Ramachandra, M., Ambudkar, S. V., Chen, D., Hrycyna, C. A., Dey, S., Gottesman, M. M., and Pastan, I. (1998) *Biochemistry 37*, 5010−5019.
57. Wang, G., Pincheira, R., Zhang, M., and Zhang, J. T. (1997) *Biochem. J. 328*, 897−904.
58. Julien, M., and Gros, P. (2000) *Biochemistry 39*, 4559−4568.
59. Sankaran, B., Bhagat, S., and Senior, A. E. (1997) *Arch. Biochem. Biophys. 341*, 160−169.


BI0120897